Results of Measured Data from Atomic Force Microscope on Ring Pack Performance

S.R. Bewsher [1], R. Hildyard [1], M. Mohammadpour [1], M. Leighton[1], H. Rahnejat [1], O. Knaus [2] and G. Offner [2]

[1]Wolfson School of Mechanical Engineering, Loughborough University, Loughborough, LE113TU, England
[2]AVL List GmbH, Graz, Austria

Abstract: Frictional losses of an IC engine include 40-50% contribution due to piston assembly-liner conjunction. Reduction of friction would improve fuel efficiency and decrease harmful emissions. Therefore, it is important to accurately predict the frictional losses due to viscous shear of a thin lubricant film as well as boundary friction, generated by the direct contact of real rough contiguous surfaces. Greenwood and Tripp model is used to evaluate the contribution due to boundary friction. The model requires the determination of pressure coefficient of boundary shear strength of asperities, ς, which is analogous to the asperity coefficient of friction. This should be determined through measurement, using Atomic Force Microscopy (AFM) in Lateral Force Mode (LFM). The value of ς is dependent on the combination of surface and lubricant as a system. Boundary active lubricant additives adsorb or bond to the surface asperities and affect the value of ς. The value of this coefficient also alters with the evolution of interacting surfaces through the process of wear as well as any degradation of the lubricant. The approach can be used to create a database of such values for different lubricant-surface systems, in particular for piston-liner interactions.

Keywords: Boundary friction, Atomic Force Microscopy (AFM), Lubricant-surface combination

Nomenclature

A	Apparent contact area
A_a	Asperity contact area
E'	Composite reduced elastic modulus of the contacting pair

f	Total generated contact friction
f_b	Boundary friction
f_v	Viscous friction
F_2	Statistical function
$F_{5/2}$	Statistical function
h	Lubricant film thickness
p	Gauge pressure
U	Sliding velocity
V	Lateral velocity (speed of side leakage flow)
$\vec{V}$	Velocity vector

Greek Symbols

ζ	Number of asperities per unit area of contact
η	Dynamic viscosity of the lubricant
κ	Average asperity tip radius of curvature
K	Conformability coefficient (factor)
σ	RMS composite surface roughness
ς	Pressure coefficient of boundary shear strength of asperities
τ	Shear stress
τ_0	Eyring shear stress

1-Introduction

The reduction of friction is critical for the automotive industry in order to improve the overall system efficiency, reduce fuel consumption and prevent wear of contacting surfaces. The approach is also driven by increasingly stringent global emission regulations, requiring more efficient internal combustion (IC) engines. Frictional losses account for 15-20% of the overall losses in IC, including the conjunctions between the piston and cylinder liner. These have been found to be the major contributor to the frictional power losses (40-50%) [1]. Lubrication and treatment of surfaces are well established methods of reducing the frictional losses.

Viscous friction of thin films is generated through shear [2], thus, the rheology of the lubricant, principally its viscosity, as well as its physical composition are the main areas for development of lubricant load carrying capacity. Current lubricants used in IC engines are subject to a large range of contact and operating conditions, whereby the reduction of lubricant viscosity has been seen as the most effective way to reduce in-cycle friction in hydrodynamic conjunctions such as that of the piston compression ring to liner contact. However, reduced viscosity results in a reduced load carrying capacity. This can have the negative effect of allowing the contiguous surfaces to interact directly at higher loads. Also, reducing lubricant viscosity in order to reduce viscous shear is constrained by the high pressures generated in contact conjunctions elsewhere in the engine, subjected to high elastohydrodynamic pressures, such as in the valve train system [3]. Consequently lubricant manufacturers use a multitude of additives, requiring a lubricant-surface system approach.

The term asperity is used to describe the unevenness of surfaces. It originates from the Latin ‘asper’ meaning rough. No surface is truly smooth and free of asperities. At an atomic level even those surface which have undergone post process finishing, such as polishing to remove surface roughness, comprise rugged edges and features. Real solids have rough surfaces and make contact only at isolated points where the asperities on the two mating surfaces come together. This is equally true whether the apparent contact area is macroscopic, as in the contact of two nominally flats, or microscopic, as in the contact of two rough spheres [4].

Greenwood and Tripp [4] adopted Hertzian contact mechanics [5] which is for localised contact of smooth ellipsoidal solids of revolution, and extended it to include the real rough surface topography.

Greenwood and Tripp [6] considers surface roughness between two plane surfaces for simplified asperity geometry and an assumed Gaussian distribution of peak heights. They also conducted an analysis on rough spheres, showing that results of classical Hertzian were not valid for low loads with low effective generated pressures.

To predict sliding temperatures or thermal resistance it is not sufficient to use just the total area of contact as the number and size of each contact is important [6]. It has been found that despite the heights of different asperities being random, the peak height distribution of these heights is close to Gaussian, in particular for ground and grit-blasted surfaces. It is also reported that the peak height distribution for worn surfaces is usually non-Gaussian. However, once the surfaces are in contact the heights of the asperities which do not touch are unimportant, so a Gaussian distribution is still reasonably valid. In all cases the area of real contact is almost proportional to the load and the load-compliance curve is almost straight on a log (load)-linear compliance plot, with a slope such that a movement of one standard deviation of the joint peak height distribution gives a load increase by a factor of about 50 [6]. A further assumption made by Greenwood and Tripp [6] is an average asperity tip radius and an average indentation depth at given separations with the mutual approach of rough counter faces. The Greenwood and Tripp model predicts the area occupied by asperities, the load carried by them and consequently the average asperity contact pressure. A representative model for friction calculations also requires the determination of pressure coefficient of boundary shear strength of asperities, ς, which is analogous to coefficient of friction at asperity interaction level. This should be determined through measurement. In the current study, an AFM is used in the lateral mode. The value of ς depends on the combination of the fully formulated lubricant and the surfaces in contact as well as the working conditions. It also depends on the working history of the parts as they are exposed to different conditions as the lubricant additives are adsorbed/bonded to them.

2-Asperity Contact Model

The overall friction is made up of viscous shear of a thin film of lubricant, f_v, and the direct interaction of rough counter face surfaces, f_b, thus:

$$f = f_v + f_b \quad (1)$$

The boundary friction caused by the asperities is obtained using [7]:

$$f_b = \tau_0 A_a + \varsigma W_a \quad (2)$$

The shear strength of asperities, ς, corresponds to the softer of the two counter faces (in this case the liner material). The procedure is described in detail by Styles et al. [8]. τ_0 is the Eyring shear stress of the lubricant [9], normally obtained through high shear viscometry.

The Greenwood and Tripp asperity contact model [6] has been used to represent the part of the load which is carried by the asperities as:

$$W_a = \frac{16\sqrt{2}}{15}\pi(\zeta\kappa\sigma)^2\sqrt{\frac{\sigma}{K}}E'AF_{5/2}(\lambda) \quad (3)$$

$\zeta K\sigma$, the roughness parameter. It is found by analysing the surface topography and σ/K is a measure of a typical asperity slope [10].

The total area of asperity tips in the apparent contact area is required to calculate equation (2). A_a is found as [4, 6];

$$A_a = \pi^2(\zeta K\sigma)^2\sqrt{\frac{\sigma}{K}}AF_2(\lambda) \quad (4)$$

The viscous friction is calculated as:

$$f_v = \int\int \tau dxdy \quad (5)$$

where the shear stress τ is obtained as:

$$\tau = \left|-\frac{dp}{dx}\vec{\nabla}p\frac{h}{2} + \frac{\eta U\vec{V}}{h}\right| \quad (6)$$

3-Utilised Lubricants and Sample Surface

It is of important to determine the lubricant rheology and physical chemistry alongside the surface material properties and topography in order to calculate friction in any contact, including the piston compression ring-liner conjunction.

Commercial lubricants are made up of various additive packages, whereby each is designed to achieve a predefined function. The additive packages typically make up 25% of the overall lubricant mass, optimising the performance of the base oil [11]. The main functions are reducing friction, removal of contaminants, including soot in the case of engine cylinders, formation of a protective barrier between moving contacting parts and also as coolants. Other additives such as detergents, dispersants, anti-wear, antioxidants and viscosity modifiers are commonly used to achieve the desired performance level. All these additives react with the contacting surfaces.

Of interest in this paper are the role of anti-wear and friction modifier species, because they directly affect friction. For example, Zinc dialkyldithiophosphate (ZDDP) is typically added to the engine base oils to reduce wear. It is necessary to balance the level of ZDDP with a dispersant to prevent sludge formation in the engine, thus having a high level of ZDDP would require more dispersants in the engine giving better performance against wear and sludge [11]. However, deposits of ZDDP tend to increase friction. They also interact with friction modifiers as an additive to reduce friction [12, 13]. Therefore, the complex interaction of boundary active elements in the formulated lubricants affect the tribo-film formation on the counter face contacting surfaces, which in turn affect the value ς. Furthermore, lubricant degradation can also occur owing to the prevailing conditions such as oxidation. Therefore, antioxidants are also used in all commercial lubricants. The surface chosen for this study is a piston liner shown in Figure 1. Liner material properties can be found in Table 1. A section of a liner, having undergone running-in process through representative engine testing is used.

Table 1: Liner Material Properties

Property	**Value**	**Unit**
Elastic modulus	120	GPa
Poisson ratio	0.28	-
Hardness (HV)	2325	MPa
In engine running time	105000	Miles

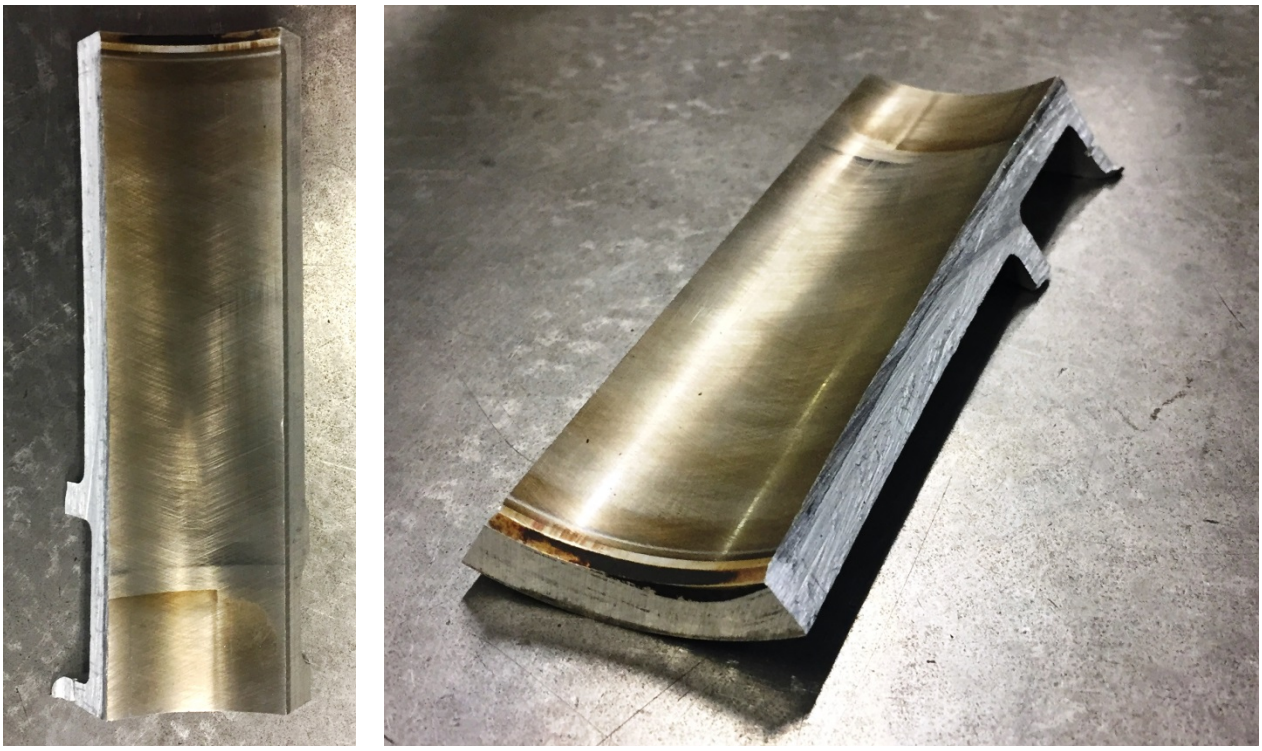

Figure 1: The cut out section of a cylinder liner

The lubricant used for the wet AFM is an off-the-shelf, fully formulated Mobil Super 3000 5W-20 motor oil which was originally used in the engine test during the running-in time.

Four different areas on the liner test piece are measured to determine the value of ς as it is expected that the competition between the lubricant additives, mainly the anti-wear and friction modifier species would result in localised conditions. An implication of this is that assuming a constant value for ς, as is usually the case in most analyses does not fully represent the in situ conditions. Furthermore, at each locality the tribo-film is subject to evolution and the value of ς would also evolve accordingly. This can be observed by comparison of results of a run-in liner with a new untested one. The various positions on the liner test-piece investigated are (figure 2):

Zone 1: This represents the area between the top compression ring and the scraper ring when at the top dead centre. This region should be subject to starvation and boundary regime of lubrication minimum sliding velocity in piston reversal.

Zone 2: This represents the area between the scraper ring and the oil control ring at the top dead centre.

Zone 3: This represents the area between the top compression ring and the scraper ring at the bottom dead centre with minimum contact pressure and low sliding speed.

Zone 4: This represents the area between the scraper ring and the oil control ring at the bottom dead centre.

Figure 2: Liner sample prepared for AFM measurement with the defined Zones 1-4

Thus, from equation (2) the remaining parameters which need to be determined in order to obtain boundary friction contribution are τ_0 and ς. This feasibility study focuses on finding the specific ς values related to this particular piston cylinder liner conjunction and the selected lubricant. Therefore, the results are only be applicable for similar oil-surface combination with a similar part history.

4-Experimental Procedure -*Friction Measurements*

An AFM is used in the lateral force mode (LFM) to determine the coefficient of boundary friction [2, 8, 14] from different zones of the cylinder liner specimen (Figure 3). LFM requires the calibration of a cantilever contact AFM probe for friction measurements [8, 15]. The specification of the AFM probe used is provided in Table 2. In the current study a Bruker DNP-10 probe with 4 tips is used. Each tip is located on a separate cantilever. However, only tip A with a spring constant of 0.120Nm^{-1} and a tip radius of 20nm is used. The parameters used for the LFM mode are listed in Table 3. The same calibration is carried out for both dry and wet AFM measurements. A syringe is used to add the lubricant creating a meniscus around the tip holder a sufficient distance away from the tip to avoid generation of meniscus forces.

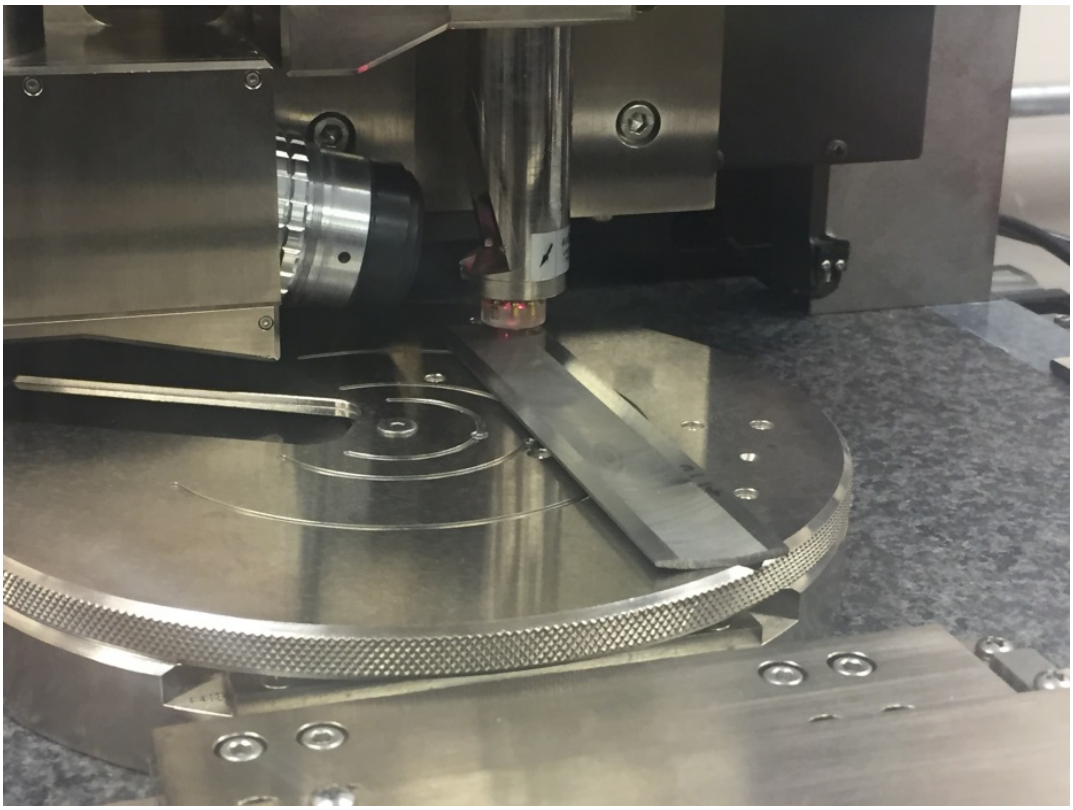

Figure 3: Liner sample undergoing AFM measurement

Table 2: Specification of the AFM probe

Model	**DNP-10**
Material	Non-Conductive Silicon Nitride
f0	50-80kHz
K	0.350Nm-1
Tip radius	20nm

Table 3: AFM settings for LFM

Parameter	Value
Scan size	4μm
Scan rate	2Hz
Samples/line	1024
Aspect ratio	4
Integral gain	2V
Proportional gain	3V
Deflection set point	0V
Scan angle (Friction)	90°

5-Results and Discussion

Determining the coefficient of boundary shear strength, ς, under dry and wet contact conditions

The contact friction of the liner specimen is measured under dry contact conditions over a range of applied loads. Figure 4 shows a graph, where the gradients of each line represent the value of ς for each of the pre-defined zones 1-4.

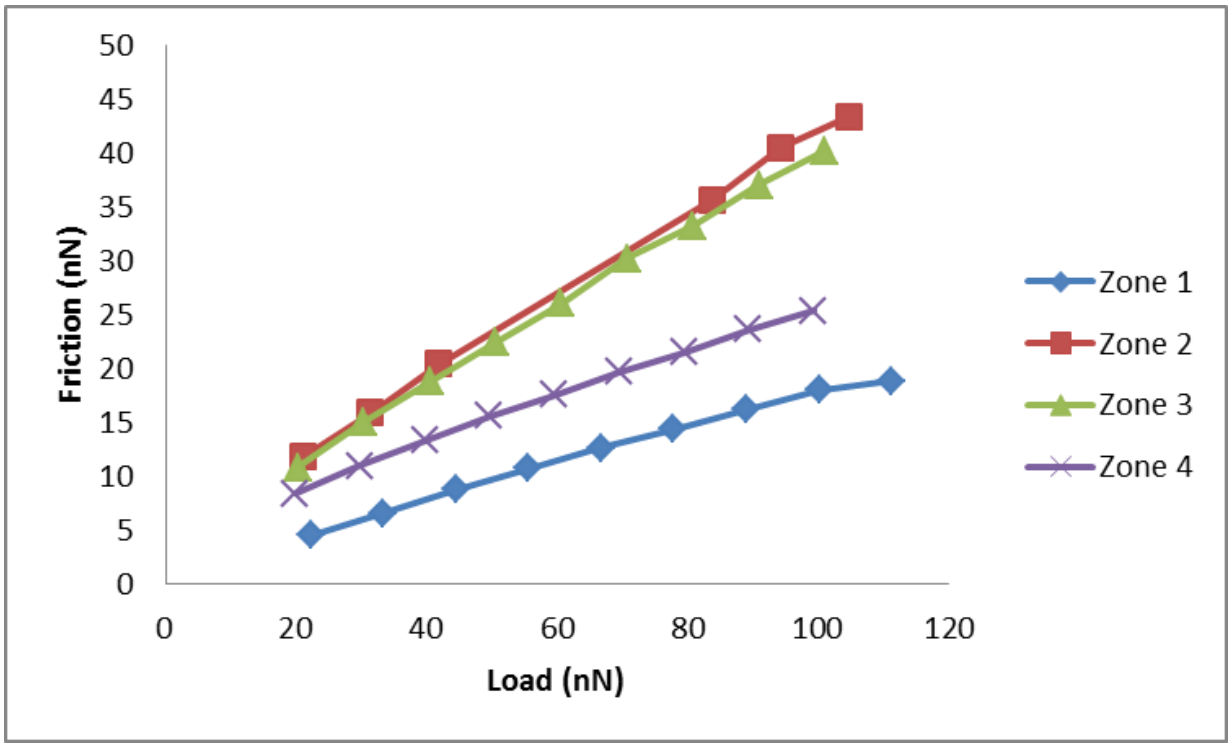

Figure 4: Friction vs load for Zones 1-4 under dry conditions as measured with LFM.

It can be seen that the Zone 1 has the lowest coefficient of boundary friction ($\varsigma = 0.164$). Zone 4 also has a relatively low coefficient of boundary friction ($\varsigma = 0.212$). Zones 2 and 3 have similar coefficients of boundary friction ($\varsigma = 0.365$ and 0.363 respectively). The graphs were from results of scans of the specimen surface, measuring 1024x256 data points across an area of 4 μm x1μm.

In order to determine the lubricant effect upon generated friction under LFM conditions, wet LFM is performed on Zones 1 and 2. Figure 5 shows the resultant friction vs. load graph from the scanned areas.

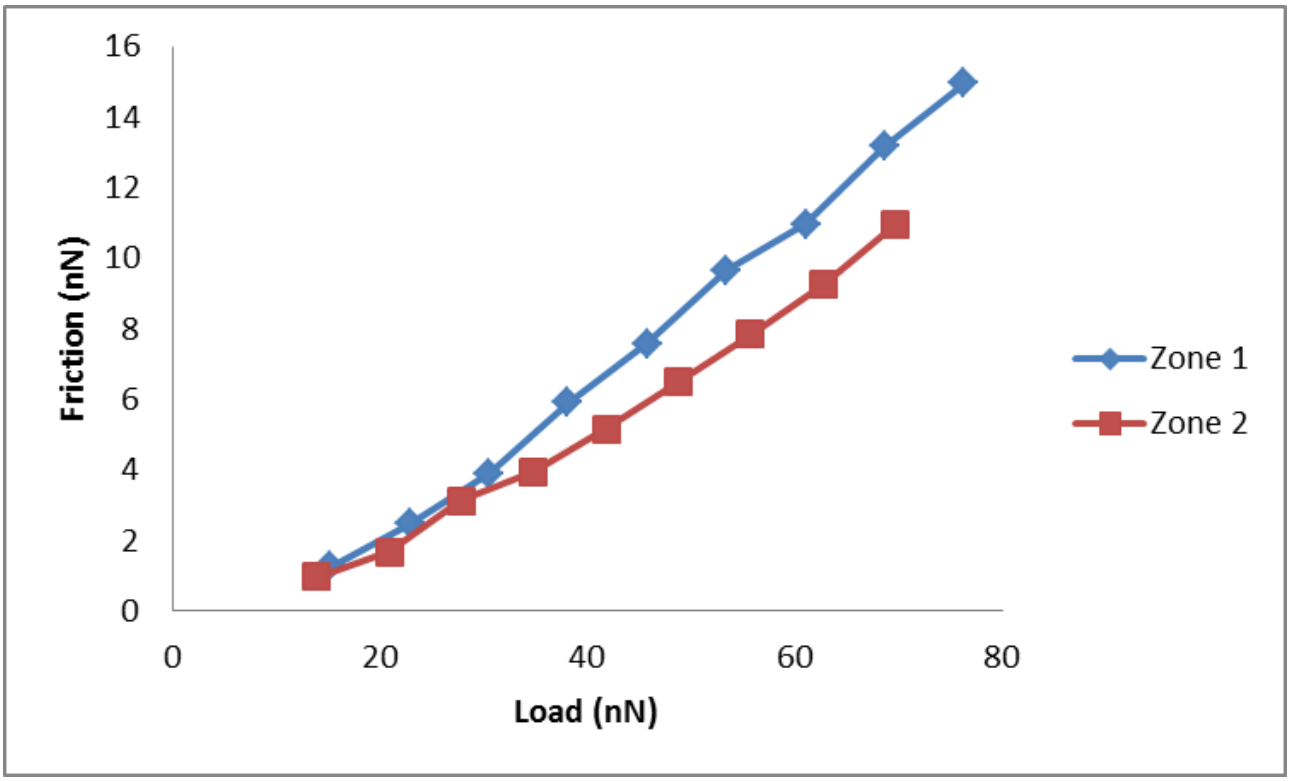

Figure 5: Friction vs load for Zones 1 and 2 under wet conditions as measured with LFM

Figure 5 shows that Zone 1 has a higher coefficient of boundary friction ($\varsigma = 0.229$) than Zone 2 ($\varsigma = 0.179$). Again, the results are from scans of the specimen surface, measuring 1024x256 data points across an area of 4μm x1μm.

An interesting observation is the increase of the coefficient of friction in Zone 1 with the lubricated contact. In order to ensure the accuracy and validity of this observation, further measurements are undertaken under dry contact conditions with scans of the surface measuring 256x256 data points over an area of $1\mu m^2$. Averaging the gradients of the 5 measurements (Dry 1-5) it is found that the coefficient of dry boundary friction remains almost unchanged at 0.168. These results show that the increase in Zone 1 under lubricated condition is due to an expected physical reason, most probably due to deposition of present ZDDP in the lubricant, having enhanced friction due to the formation of a wear resistant coating. High contact pressures under LFM conditions and thus generated high flash temperature are sufficient to form patches of ZDDP film on the surface of the specimen. This finding is

also in line with the observations in [12]. Nevertheless, further investigation of surface is required, such as through XPS measurement.

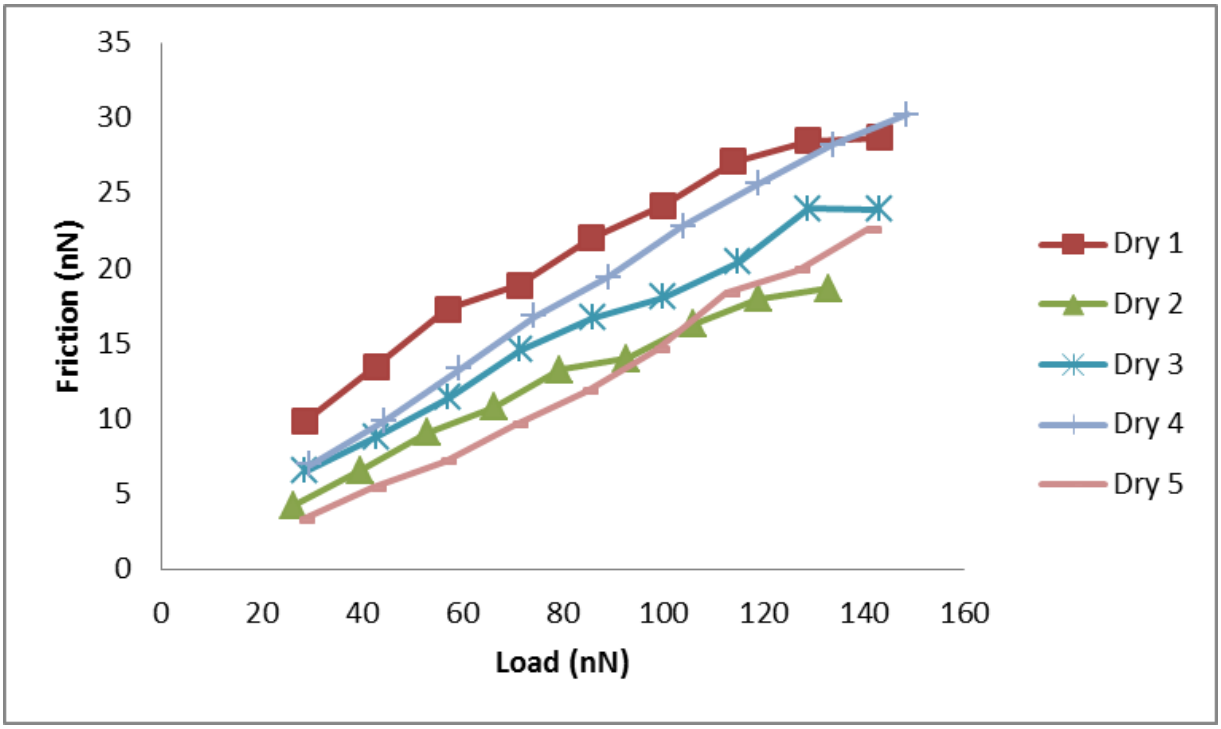

Figure 6: Friction vs load for Zone 1 under dry conditions as measured with LFM.

Another observation is that the dry measurements show scattered results around two distinct gradients, one 0.16 and the other 0.19 (Figure 6). This finding can be explained by uneven deposition of additives on the surface. ZDDP forms in patches on the surface of specimen. This observation shows the necessity of employing a statistical method in implementing an average value for ς over given regions of contact.

6-Conclusion

The study has used a fully formulated off-the-shelf lubricant with an additive package combined with the actual surface of a run-in cylinder liner from a representative engine test, as opposed to the previous methods using base oils with especially manufactured new samples or partially formulated lubricants. It is shown that the coefficient of friction varies locally and is not constant over the different

regions of contact under both dry and lubricated conditions. Therefore, when applying ς to the Greenwood and Tripp model to calculate boundary friction, it is not a representative assumption to use a single value.

Due to the uneven deposition of a tribo-film on the surface, two distinct regions corresponding to areas (with and without deposits) can be identified. This is clearly the case for some additives which form patches on the surfaces such as ZDDP. Therefore, some statistical method is required in order to implement these results in a single predictive model.

Acknowledgements

The authors would like to express their gratitude the Engineering and Physical Sciences Research Council (EPSRC) and AVL List for the financial support extended to this research.

References:

[1]- Tung, S.C. and McMillan, M.L., “Automotive tribology overview of current advances and challenges for the future”, Tribology Int., 2004, 37: 517-536.

[2]- Leighton, M., Nicholls, T., De la Cruz, M., Rahmani, R. and Rahnejat, H., “Combined lubricant-surface system perspective: Multi-scale numerical-experimental investigation”, Proc. IMechE, Part J: J. Engineering Tribology, 2016; 0(0): 1-15, DOI: 10.1177/1350650116683784

[3]- Kushwaha, M. and Rahnejat, H., "Transient elastohydrodynamic lubrication of finite line conjunction of cam to follower concentrated contact", J. Phys., D: Applied Physics 35(21), 2002: 2872.

[4]- Greenwood, J.A. and Tripp, J.H., “The Elastic Contact of Rough Spheres”, Journal of Applied Mechanics, 1967; 34 (1): 153-159.

[5]- Hertz, H., “Miscellaneous Papers by H. Hertz”, London: Macmillan, 1896.

[6]- Greenwood, J.A. and Tripp, J.H., “The contact of two nominally flat rough surfaces”, Proc. IMechE, 1970-1971, 185: 625-634.

[7]- Briscoe, B.J., Scruton, B. and Willis, F.R., “The shear strength of thin lubricant films”, Proc. Roy. Soc. London, A-333, 1973, pp. 99-114.

[8]- Styles, G., Rahmani, R., Rahnejat, H. and Fitzsimons, B., “In-cycle and life-time friction transience in piston ring–liner conjunction under mixed regime of lubrication”, Int. J. Engine Research, 2014, 15(7): 862-876.

[9]- Eyring, H., “Viscosity, plasticity and diffusion as examples of absolute reaction rates”, J. Chem. Phys., 1936, 4: 283.

[10]- Gohar, R. and Rahnejat, H., “Fundamentals of Tribology”, Imperial College Press, London, 2008.

[11]- Rudnick L.R., “Lubricant Additives: Chemistry and Applications”, Second Edition, CRC Press, 2009.

[12]- Taylor, L.J. and Spikes, H.A., “Friction-enhancing properties of ZDDP antiwear additive: part II—influence of ZDDP reaction films on EHD lubrication”, Tribology Transactions, 2003, 46(3):310-314.

[13]- Wan, Y., Cao, L. and Xue, Q., “Friction and wear characteristics of ZDDP in the sliding of steel against aluminum alloy”, Tribology International. 1997, 30(10):767-772.

[14]- Chong, W. and Rahnejat, H., “Nanoscale friction as a function of activation energies”, Surface Topography: Metrology and Properties, 2015. 3(4): p. 044002.

[15]- Buenviaje, C.K., Ge, S.R., Rafailovich, M.H. and Overney, R.M., “Atomic force microscopy calibration methods for lateral force, elasticity, and viscosity”, In MRS Proceedings, Cambridge University Press, 1998, 522: 187.